International Journal of Biological Macromolecules 117 (2018) 427–434

Contents lists available at ScienceDirect

International Journal of Biological Macromolecules

journal homepage: http://www.elsevier.com/locate/ijbiomac

Gelatin-alginate coacervates for circumventing proteolysis and probing intermolecular interactions by SPR

Hui-Chong Lau, Seonghee Jeong, Aeri Kim *

College of Pharmacy, CHA University, 521 CHA Bio Complex, 335 Pangyo-ro, Bundang-gu, Seongnam-si, Gyeonggi-do 13488, Republic of Korea

ARTICLE INFO

Article history:
Received 24 February 2018
Received in revised form 15 April 2018
Accepted 15 May 2018
Available online xxxx

Keywords:
Coacervate
Gelatin
Alginate
Protein encapsulation
Proteolytic degradation
SPR biosensor

ABSTRACT

Complex coacervates based on natural biopolymers have been explored as a protein delivery system to provide controlled release of loaded protein and circumvent the proteolytic degradation in chronic wounds. The coacervates composed of gelatin A (GA) and sodium alginate (SA) were optimized with respect to turbidity, size, zeta potential, and polydispersity index. Bovine serum albumin (BSA), a model protein, was effectively encapsulated in the coacervates, resulting in protection from trypsin digestion and controlled release. In contrast, EGF was not encapsulated in the same coacervates. Striking difference in the encapsulation efficiencies of BSA and EGF, despite their similar net charges, was attributed to their different levels of binding to GA based on the surface plasmon resonance (SPR) biosensor analysis. In conclusion, GA and SA coacervates can protect the encapsulated protein from proteolytic degradation, demonstrating its potential as a delivery system in the chronic wounds. SPR biosensor is proposed as an analytical tool to study the interactions between polymers and proteins in association with encapsulation efficiency in complex coacervation. The results of EGF studies suggested that GA was not a suitable polymer for EGF encapsulation and therefore, further investigation would be needed to find suitable polymer systems for improved encapsulation efficiency.

1. Introduction

In chronic wounds such as diabetic foot ulcer (DFU), high levels of inflammatory cells lead to the elevated levels of proteases that appear to degrade extracellular components, growth factors, and other proteins. Elevated levels of proteases in the chronic wound environment can also lead to degradation of the growth factors topically applied for wound healing purposes [1,2]. Hence, treatment options with growth factors for chronic wounds would exhibit limited efficacy unless the drug delivery system is designed to circumvent protease degradation in the wound bed. In addition to improved efficacy, ease of administration and prolonged storage stability at ambient conditions would benefit both patients and care givers. Maintaining the integrity of the protein as its native form is vital to retain functional activity of the protein before being delivered to the patients [3]. An advanced topical delivery system satisfying above mentioned features for chronic wounds is yet to be developed.

In light with the limitations of topical delivery system for chronic wound healing, a number of complex coacervate systems have been studied as a topical delivery platform with the hypothesis that coacervate would reduce the degradation of encapsulated protein and maximize the release efficiency at wound beds. For example, a synthetic positively charged polymer, polyethylene adipate, and heparin were used as polyelectrolytes complex to carry the desired growth factors such as epidermal growth factor (EGF) and vascular endothelial growth factors (VEGF) [4–10]. Complex coacervate is a liquid-liquid separation system held together mainly by electrostatic interactions between polyelectrolytes [11–14]. It often appears in the form of droplets in spherical shape and resembles the form of emulsion of dispersant and the size varies from micro to nanometers. Upon formation, the complex will appear in two phases, dilute and dense phases. In the past, complex coacervate has been often applied in food industry and recently, coacervate in drug delivery system (DDS) has been reported for application in the DFU, inflammation, and even in the cardiovascular diseases [8,10,15,16]. Synthetic biodegradable polymers such as polypeptides, poly (L-lysine), and poly (D/L-glutamic acid) were used to encapsulate BSA as potential DDS in biomedical application [17]. However, information on the coacervate using natural biopolymers in biomedical science is still limited. Hence, further investigation on the use of natural biopolymer based coacervate can potentially provide an alternative platform for topical wound treatment.

In the present study, we aimed to develop coacervate composed of natural biopolymers, sodium alginate (SA) and gelatin A (GA), to circumvent encapsulated proteins from protease in the wound bed. SA and GA were selected as polyelectrolytes for coacervate system because of their well-known wound healing effect [4,18–20]. GA is also known to carry anti-inflammatory properties, which can accelerate wound

* Corresponding author.
E-mail address: arkim@cha.ac.kr (A. Kim).

https://doi.org/10.1016/j.ijbiomac.2018.05.093
0141-8130/

healing activity [21,22]. The coacervates composed of sodium alginate and gelatin A (GA/SA) were optimized with respect to the physical properties such as turbidity, size, zeta potential, and polydispersity index (PDI). In addition, BSA was selected as a model protein to evaluate the encapsulation efficiency in the present GA/SA coacervate. Encapsulation of EGF was then measured to evaluate the feasibility of the present GA/SA coacervate as a drug delivery system to chronic wounds. Despite the previous reports on the use of coacervate system in biomedical research, science behind the system remains poorly understood. Another aim of the present study was to use SPR biosensor to analyze the interactions between proteins and biopolymers by determining their specificity and kinetics in real-time, in particular, to better understand the encapsulation efficiency of different target proteins, BSA and EGF. To date, there is no report on the use of SPR biosensor to study the GA/SA coacervate encapsulating BSA or EGF.

2. Materials and methods

2.1. Materials

Sodium alginate was from Daejung (Gyeonggi-do, Korea), Korea. Gelatin A (Gel strength 300, and 90–110) was obtained from Sigma-Aldrich (St. Louis, MO, USA), Fluorescein isothiocyanate (FITC) was purchased from TCI (Tokyo, Japan). Phosphate buffer solution (PBS) buffer was obtained from Gibco, USA. Bovine serum albumin (BSA) was obtained from Milipore, (Bedford, MA, USA). Epidermal growth factor (EGF) was a gift from Daewoong Pharmaceutics Company, South Korea. Sephadex™ G-50 Fine, CM5 sensor chip, amine coupling kit, 10 mM sodium acetate buffer at different pH, 50 mM NaOH, ethanolamine were obtained from GE Healthcare, Bio-Sciences AB, (Uppsala, Sweden).

2.2. Formulation and characterization of coacervate

2.2.1. Coacervate formulation based on gelatin and sodium alginate to encapsulate BSA and EGF as model drugs

0.5% (w/v) of gelatin A (GA), 0.5% (w/v) of sodium alginate (SA), and 1 mg/mL of BSA were prepared as a stock solution for fabrication of BSA coacervate. To optimize the formation of BSA coacervate, GA:SA mixture at different volume ratios (3:1, 4:1, 5:1, 6:1) v/v and BSA solution of 100 μg/mL were added sequentially into a 1.5 mL tube to a final volume of 1 mL. The pH of each formulation was adjusted to determine the efficiency of coacervation. Optimal coacervate was chosen based on turbidity and minimal formation of precipitates among various pH conditions. Each vial of formulation was incubated at room temperature for 30 min for equilibrium. Coacervate was concentrated when necessary, via centrifugation at 14,000 rpm for 10 min in a bench top centrifuge (Labogene, Seoul, Korea) for collecting the pellet. GA:SA with the highest encapsulation efficiency was used in the subsequent studies. EGF coacervate was prepared using the same formulation developed for BSA coacervate. EGF solution of 100 μg/mL was used to prepare the EGF coacervate with GA and SA at several ratios (3:1, 4:1, 5:1, and 6:1).

2.2.2. Physical characterization of protein coacervate

The zeta potentials of proteins and optimized coacervate formulation were measured using Zetasizer Nano-ZS (Malvern Instruments, Worcester, UK). The measurement was based on electrophoretic light scattering method. In brief, 1 mL of 100 μg/mL sample in distilled water was transferred into a folded capillary cell (Malvern Instrument, DTS 1060C) using a disposable syringe. Three runs were done with each run consisting of 10 single measurements. The size distribution and polydispersity (PDI) of the BSA coacervate were measured using dynamic light scattering (DLS) on Zetasizer Nano-S (Malvern Instruments, Worcester, UK). All measurements were repeated at least twice. Turbidity of the BSA and EGF coacervates (pH 4–8) at 600 nm was measured in 1 mL cuvette using SpectraMax 384 microplate reader (Molecular Devices, Sunnyvale, USA). All the measurements were done in triplicate.

2.2.3. Preparation of FITC labelled BSA

Fluorescein isothiocyanate (FITC) labelled BSA (FITC-BSA) was prepared according to the manufacturer's protocol. The FITC-BSA was then filtered through a Sephadex™ G-50 Fine gel matrix with an exclusion limit of 20,000–50,000 to collect the FITC-BSA. The FITC-BSA was then used for further quantification of encapsulation, release studies, and proteolysis activity.

2.2.4. Encapsulation and loading efficiency

For qualitative estimation of encapsulation efficiency, the supernatant and pellet of the coacervate after centrifugation were analyzed using sodium dodecyl sulfate polyacryclamide gel (SDS-PAGE). In brief, concentrated complex coacervate was centrifuged at 14,000 rpm for 10 min (Labogen, Seoul, Korea). After collecting the supernatant, pellets were dissolved in PBS. A total of 20 μL each of pellet and supernatant were heated at 100 °C for 10 min and loaded onto 15% SDS-PAGE. Silver stain was carried out to determine the encapsulated and free protein in pellet and supernatant respectively.

For quantitative measurement of the encapsulation efficiency, the percentage of FITC-BSA encapsulated in the coacervate droplet was calculated as follows:

$$\%\text{Encapsulation efficiency} = \left[\left(\text{Total BSA} - \text{Free "unencapsulated BSA"/Total BSA}\right)\right] * 100$$

Free "unencapulated BSA" was quantified by measuring the fluorescence intensity of FITC-BSA in the supernatant after centrifugation of the coacervation reaction solution at 14,000 rpm for 10 min (Labogene, Seoul, Korea). The fluorescence intensity was measured using Multimode Microplate Reader (Molecular Devices, Sunnyvale, USA) with excitation at 495 nm and emission at 595 nm.

Loading efficiency was calculated based on the BSA encapsulated and the total dried weight of the complex. Encapsulated BSA was determined from the free "unencapsulated BSA" quantified above.

$$\%\text{Loading efficiency} = [\text{Encapsulated BSA/polymer complex dried weight}] * 100$$

Different volume ratios of GA:SA were used to determine the encapsulation efficiency and loading efficacy of BSA coacervate.

2.2.5. Proteolytic digestion of BSA in the coacervate relative to free BSA

BSA coacervate and physical mixture were prepared at GA:SA ratio 4: 1 and 100 μg/mL BSA as described in Section 2.2.1. BSA-coacervate, physical mixtures of BSA and free BSA were prepared with GA:SA ratio 4:1 without and with 0.5 M acetic acid 5 μL, respectively. Samples were incubated at 37 °C with 100 rpm for 2 h in the presence of trypsin (weight ratio of BSA: trypsin, 1:1 and 1:4) to determine the protection of BSA in the coacervate from degradation compared to free BSA and physical mixture. To adjust the pH of BSA-coacervate samples which can impact the trypsin activity, 50 mM NaOH 7 μL was added in the sample tube. All samples were analyzed using 12% SDS-PAGE to determine the protection ability of BSA-coacervate.

2.2.6. Freeze-drying of coacervate

Concentrated BSA coacervate obtained by centrifugation of the coacervation reaction solution in 1.5 mL tubes followed by removal of the supernatant were first frozen at −80 °C overnight and then dried using a freeze dryer (Gperon, Korea).

2.2.7. In vitro release test

The release rate of the freeze-dried coacervate was tested using 24 Transwell® Permeable Support 0.4 μM (Costar, Kennebunk, ME, USA). 1 mL of PBS was added into the multiwell plate as the release media and each freeze-dried sample was placed into the Transwell inserts. Each plate was then incubated at 37 °C with 100 rpm for different time points (3, 6, 9, 12, 24 h). The release rate was measured and calculated based on the formula below:

$$\%\text{release} = (\text{protein released at time T}/\text{initial protein loaded}) * 100$$

2.3. Analysis of interactions between polymers and model proteins by SPR

Interactions between GA and {SA, BSA, or EGF} were evaluated using Biacore SPR biosensor T200 (GE Healthcare, Bio-Sciences AB, Uppsala, Sweden). All the SPR experiments were conducted at 25 °C using CM5 sensor chips (GE Healthcare, Bio-Sciences AB, Uppsala, Sweden). In addition to providing evidence of the binding ability, kinetics was also investigated to determine the interactions between the polymers and BSA. Prior to GA immobilization, binding and kinetics analysis, pH scouting was first carried out. The GA bound to the surface of sensor chip was used for subsequent binding and kinetics analysis. Binding experiment and kinetic analysis were conducted to analyze the association and dissociation properties of SA, BSA, and EGF. Details of each step are described below:

2.3.1. pH scouting

Prior to covalent immobilization of the GA on the sensor chip, optimal pH was identified by "scouting", as follows. Solutions of GA in 10 mM sodium acetate with pH values of 4.0, 4.5, 5.0, and 5.5 were prepared according to the manufacturer's instruction. These samples were injected into the carboxymethyl groups of the sensor chip. The bound molecules were removed by sequential injections of 50 mM NaOH. The pH buffer with the highest level of immobilized GA on the sensor surface was chosen for the immobilization of GA with amine coupling reaction.

2.3.2. Immobilization of ligand

The chip surface was first activated using a 1:1 mixture of 0.4 M of 1-ethyl-3-(3-dimethylaminopropyl) carbodiimide (EDC) and 0.1 M N-hydroxysuccinimide (NHS), followed by covalent linking of the GA with the carboxymethyl groups of the Sensor chip CM5 surface as described by the manufacturer. The GA was prepared using optimum pH of 10 mM sodium acetate buffer as described before under the pH scouting section. The unused activated sensor chip surface was blocked with 1 M ethanolamine. Reference surfaces were prepared in the same manner, except that all carboxyl groups were blocked and no ligand was added. The final concentration of bound ligand, expressed in RU, was calculated by subtracting the reference RU from the sensing RU. The immobilization protocols were followed as illustrated in Supplementary materials, Table S1.

2.3.3. Binding and kinetic analysis

Binding test was carried out to determine the interaction between GA and {SA, EGF, or BSA}. PBS at pH 4.5 was used as both running and analyte-dilution buffer. SA and BSA at various concentrations were used to flow over the immobilized-GA surface and the binding response of analyte to ligand was recorded. The chip surface was regenerated by removing the analyte with a regeneration buffer. Optimization was carried out by using several regeneration buffer solutions at various pH (pH 7, 8, and 9). The maximum response unit (RU) with each BSA and SA indicates the level of interactions. Data were processed and analyzed using Biacore T200 evaluation software and fit globally to a 1:1 local fit binding model, A + B = AB, where A represents the injected SA, BSA or EGF, whereas B is the immobilized GA, and AB is the SA-GA, BSA-GA or EGF-GA complex formed during the reaction. Kinetics analysis was subsequently carried out to determine the association and dissociation constant. Association contact time of 420 s and 100 s of dissociation time was used in the kinetic analysis for SA. Contact time of 120 s and 100 s were used as association and dissociation time for SA. Experiments were repeated twice to verify consistency.

3. Results and discussion

3.1. Formulation and characterization of coacervate

3.1.1. Formulation

Coacervation is driven mainly by electrostatic interaction between two oppositely charged polymers. Coacervate formation in the colloid system depends on several factors such as the polymer ratio and pH. These factors are involved in the construction of polyelectrolyte complex, not only the coacervate but also the formation of aggregates or precipitates [7]. It has been reported that precipitation and coacervation conditions could be potentially overlapped in the equilibrium and then lead to false identification of coacervate [12]. Hence, fabrication of protein coacervate requires optimization of polymer ratio and pH to avoid precipitation and maximize the encapsulation efficiency.

GA has been widely used as a biopolymer and is an excellent polymer of choice in this study. It has been reported to carry anti-inflammatory properties and enhance the wound healing process [23,24]. SA serves as an anionic polymer, which is often used as a dressing material in wound healing due to its high absorption of exudates, providing a moist environment preventing the wound bed from drying [25,26]. GA becomes positively charged upon pH decrease below its pI of 7–9, and interacts electrostatically with the negatively charged carboxylic groups of manuronic and guluronic acid units in alginate, giving rise to polyelectrolytes complex. The potential difference between the two polymers was first measured to estimate the optimal ratio between GA and SA for coacervation. Stock solution for GA and SA prepared in distilled water had the zeta potential value at +8.5 mV and at −45.5 mV, respectively. As the weight percentage of GA and SA solution reduced, the zeta potential of GA became more positive whereas the zeta potential of SA became more negative (data not shown). Coacervation tends to occur when the reaction mixtures are close to neutralization. As the system pH is becoming lower than pI of GA, GA binding to SA occurs and neutralization of the negative charges on SA follows. Subsequently, this process promotes the phase separation and facilitates the formation of coacervate droplets. Previous studies by several research groups reported the use of ratio 4:1 or 3.5:1 for GA:SA for optimum coacervate formation from 1–4% (w/v) of GA and SA [27–29]. In the present study, the ratio between GA and SA ranging from 3:1, 4:1, 5:1 and 6:1 were judiciously selected based on the zeta potential values obtained during the initial coacervation screening. Encapsulation efficiency and loading capacity of coacervate with BSA based on these ratios were measured to determine the most suitable ratio for subsequent experiments.

3.1.2. Physical characterization of protein coacervate

Macroscopic images of the coacervate formed at different pH values are shown in Fig. 1a. Turbidity changes in the mixture of GA and SA upon addition of acetic acid was distinctively visible due to enhanced coacervate formation. As the pH gradually decreased, turbidity further increased until two layers formed, the lower one being accumulated coacervate [28].

Fig. 1b shows the increase of sample (GA/SA, 4:1) turbidity measured by absorbance change at 600 nm with the pH decrease which is consistent with the previous report by Elmer et al. [30]. Turbidity is represented as a reverse sigmoidal curve from pH 3–12. Upon reduction of pH, desolvation of charged polymers leads to the formation of coacervate. Samples prepared with pH >5 resulted in more precipitates. As the pH becomes lower than 5, electrostatic interactions between

(a)

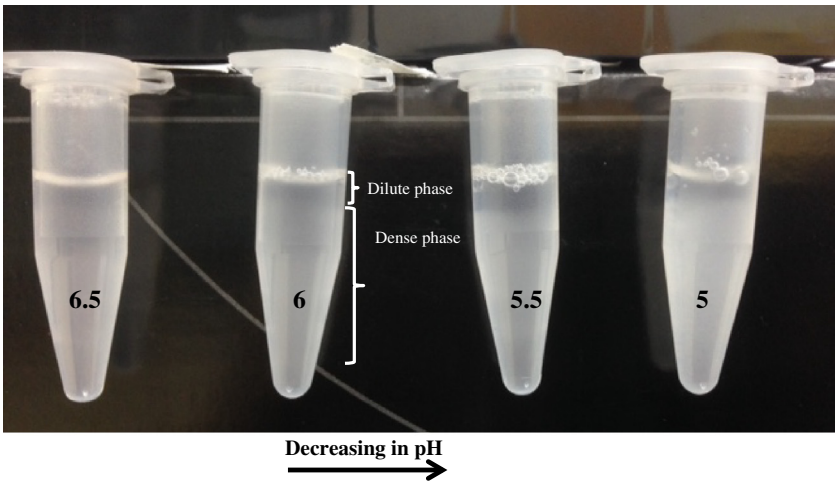

(b)

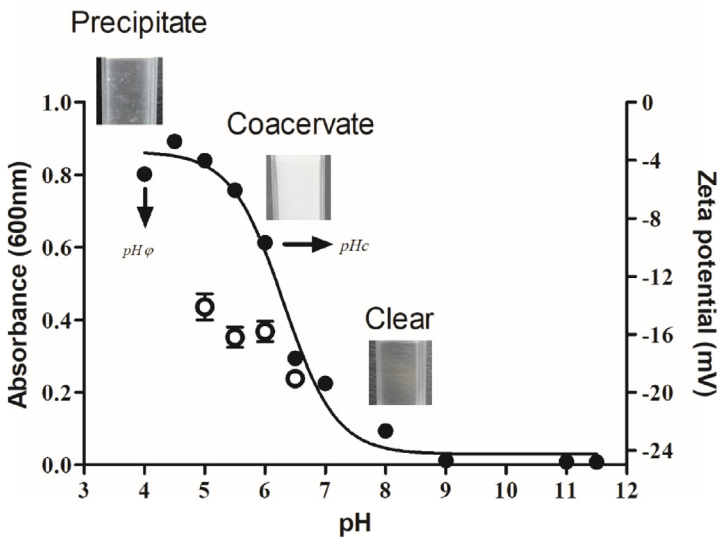

Fig. 1. (a): BSA complex coacervate at different pH values. Turbidity increased as pH decreased from 6.5 to 5.0 with addition of diluted acetic acid. (b): pH dependence of turbidity (●) and zeta potential (O) of BSA coacervate at GA:SA ratio (4:1) with 100 μg/mL of BSA. pH_c represents the pH for onset of coacervation whereas pH_φ is for precipitation.

polymers increase with expulsion of counterions, which consequently lead to the formation of precipitates [7]. pH_c and pH_φ represent the pH of the first appearance of turbidity and the occurrence of precipitate, respectively [31]. They were at pH 6.5 and at pH 4.5 for the GA:SA ratio of 4:1. For example, the reaction solution, composed of anionic polymer SA and the cationic polymer GA, turned turbid at pH 6.5 upon addition of acetic acid, indicating initiation of coacervation at this condition. As the number of hydrogen ions further increased, the electrostatic interactions among polymers of different charges also increased gradually, and the turbidity increased accordingly. As the pH was further reduced, precipitation increased and, at pH 4.5, the solution became clear after precipitates settled down.

The zeta potential of the coacervate depended on the pH (Fig. 1b). As the pH of the complex coacervate was reduced, the zeta potential value of the complex increased gradually from −19 to −14 mV. Due to precipitation upon further reduction of pH below pH_φ, the zeta potential at lower pH was not measured. Zeta potential of precipitates could be very close to zero due to the phase transition of polymers [32]. In DLS, size distribution is determined by measuring average distribution of particles based on time dependent fluctuation of scattered light intensity. The BSA coacervate prepared at pH 5.5 to 6.5 had higher polydispersity than the ones at pH 5 (Table 1). Appearance of the smaller size peak detected from the samples prepared at pH 6.5–5.5 might be due to the presence of free BSA or polymer in the mixtures. As the pH decreased to 5, the coacervate system was monodisperse with a single peak at 895 nm, PDI of 0.215, and with the average hydrodynamic size of 825.6 nm. PDI is recommended to be less than 0.6 to have unified and monodisperse distribution of sizes [6,13].

3.1.3. Encapsulation of BSA and EGF using various polymer ratios

Several ratios (3:1, 4:1, 5:1, and 6:1) of GA:SA were tested at pH 5.0. Qualitative encapsulation efficiency was determined based on the relative band intensities in SDS-PAGE of supernatants and pellets, obtained by centrifugation of BSA coacervate system (Fig. 2a) and EGF coacervate system (Fig. 2b). Multiple protein bands at 20–25 kDa belong to the free gelatin in the mixtures. BSA band at 66 kDa was observed in all the pellets of BSA coacervate but almost invisible in the supernatants, except the GA:SA (3:1) supernatant sample which showed a thin BSA band. The results suggest that BSA was encapsulated successfully and the encapsulation efficiency depended on the ratio of GA to SA. In contrast to

Table 1
Sizes distribution of GA:SA (4:1) coacervates encapsulating BSA.

GA:SA (ratio)	pH	Z average nm	Size (nm) peak 1	Peak 1 intensity (%)/volume (%)	Size (nm) peak 2	Peak 2 intensity (%)/volume (%)	PDI
4:1	6.5	895.2	906	60.8/78.6	24.9	43.9/21.4	0.6
4:1	6.0	833.5	815	85.5/5.4	32.28	15.5/52.5	0.7
4:1	5.5	853.4	853.9	58.5/92.6	20.72	41.5/7.4	0.65
4:1	5	825.6	895	100/100	–	–	0.215

Intensity (%) = percentage of intensity-weighted particle size.
Volume (%) = percentage of volume-weighted particle size.

BSA coacervate, EGF band was more intense in the supernatant than in the pellet regardless of GA:SA ratio (Fig. 2b), indicating no significant encapsulation in the coacervate. The target amount of encapsulation efficiency would depend on the particular protein of interest for encapsulation. We, however, would like to suggest that encapsulation is not sufficient qualitatively when the protein band in the pellet is less intense than that of the supernatant. Further optimization using various polymer ratios of GA and SA or GA and hyaluronic acid, salt concentration and pH adjustment did not improve the encapsulation efficiency of EGF (data not shown).

When the encapsulation efficiency was measured quantitatively using FITC-labelled BSA, complex coacervate formed at pH 5 from various ratios of GA:SA did not show significant difference in terms of encapsulation efficiency (Fig. 2c). However, GA:SA at ratios of 5:1 and

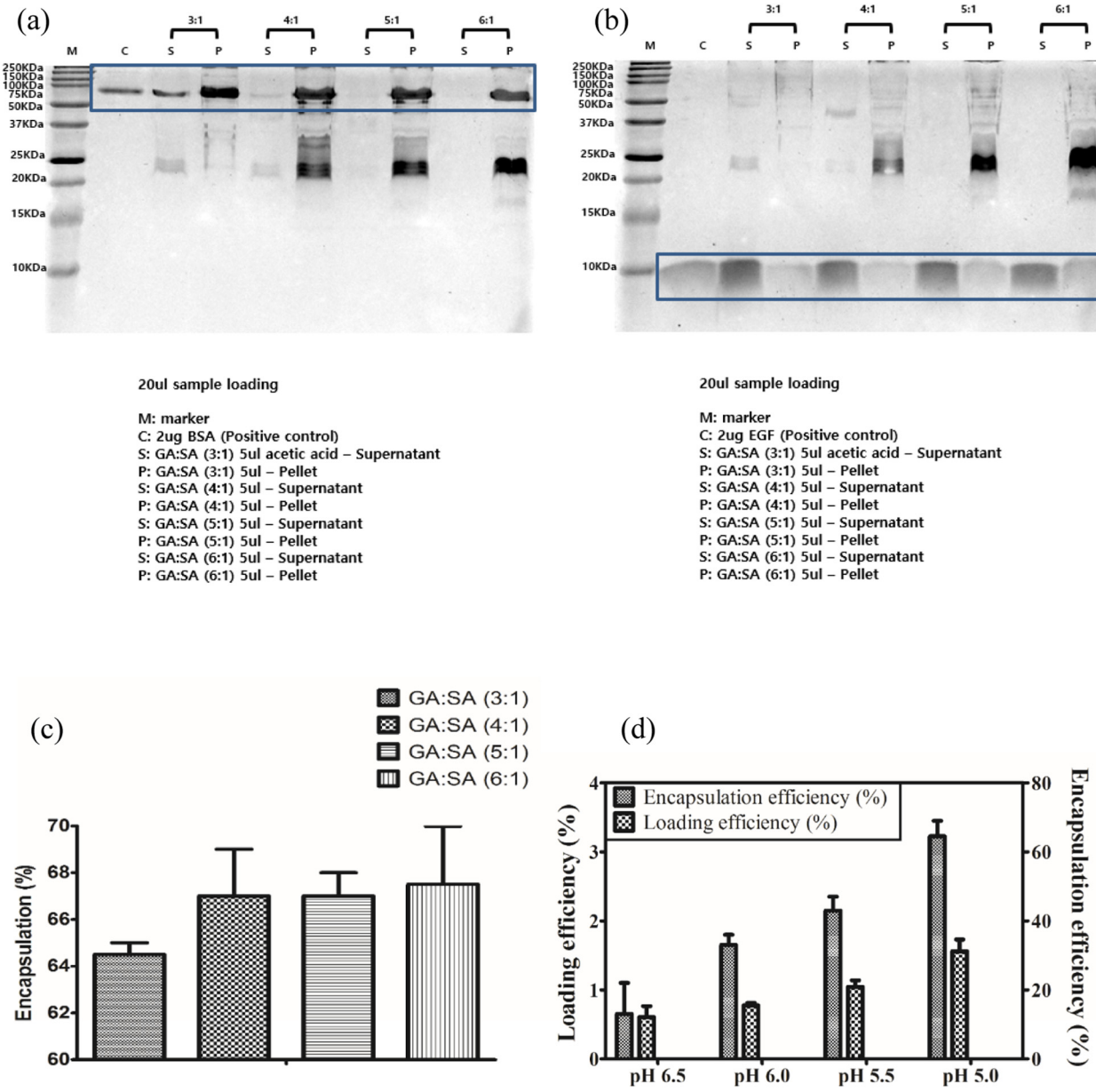

Fig. 2. SDS-PAGE of the supernatants and pellets of BSA coacervate (a) and EGF coacervate (b) at pH 5 with varying ratios of GA:SA (3:1, 4:1, 5:1, and 6: 1). (c): Encapsulation efficiency of BSA complex coacervate prepared at pH 5 with varying ratios of GA:SA (3:1, 4:1, 5:1, and 6:1). (d): Encapsulation and loading efficiency of BSA complex coacervate formulated at GA:SA ratio (4:1) at different pH (6.5–5.0).

6:1 resulted in mild precipitation at the same pH. Dependence of pH_ϕ on the polymer ratio was also observed with GA:SA ratio of 6:1 or 8:1 which showed pH_ϕ of 5.0 and 5.4, respectively (data not shown). Such higher pH_ϕ at higher GA:SA ratio compared to GA:SA (4:1) sample could be due to less negative zeta potential of high GA:SA solution. Less acid will be required to cause precipitate when the zeta potential is less negative. The coacervate system of GA:SA (4:1) showed significant precipitate formation at pH less than 5. Hence, coacervate system with pH less than 5 is not recommended for the ratio of GA:SA tested in the present study. When the pH of the coacervate system of GA:SA (4:1) was adjusted to 6.0, 5.5, and 5.0 via titration with dilute acetic acid, the encapsulation efficiency increased gradually (Fig. 2d). This suggests that BSA entrapped in the coacervate increased as positively charged GA increased with the pH change. Upon pH change to a more acidic value, more coacervates were formed due to the increased interactions of GA to the negatively charged SA and BSA. In addition, loading efficiency in the coacervate also increased gradually as the pH decreased (Fig. 2d). Hence, the BSA coacervate prepared at pH 5 with the GA:SA ratio of 4:1 was chosen for the subsequent proteolytic digestion and release studies.

3.1.4. Proteolytic digestion of BSA complex coacervate

Trypsin digestion was carried out as a model system in order to provide the evidence for protection of protein in the coacervate from proteolysis. Two different weight ratios of BSA to trypsin (1:1 and 1:4) were tested. BSA in BSA-coacervate was protected until 2 h compared to the physical mixture, whereas free BSA was almost digested in 2 h at both 1:1 and 1:4 ratios (Fig. 3). This suggests that the present GA:SA coacervate system could potentially circumvent the proteolytic degradation of encapsulated protein upon application to the wound as a topical delivery system.

3.1.5. In vitro release rate of freeze-dried coacervate

Release rate of BSA at 37 °C varied depending on the pH of the coacervates formation (Fig. 4). BSA coacervate prepared at pH 6.5–5.5 had faster release rate than the coacervate prepared at pH 5.0 for the first 12 h of incubation. The controlled release pattern of the coacervates prepared at pH 5 is consistent with the higher encapsulation efficiency at pH 5 than others pH values as shown in Fig. 2d. Taken together, the present coacervate system prepared at pH 5 can be used to achieve a sustained release pattern. BSA release from the coacervate system prepared at pH 6.5–5.5 was more than 60% during the first 6 h and then reaching almost 70% by 12 h whereas BSA coacervate prepared at pH 5 showed sustained release up to 24 h. This suggests that the coacervation condition can be modified to modulate the release rate of BSA coacervate.

3.2. SPR Biacore experiments

Fig. S1 in Supplementary materials shows a schematic diagram of tentative interaction between GA and BSA.

3.2.1. pH scouting

The pH scouting results showed that the pH buffers 4 and 4.5 had higher immobilization of GA on sensor chip than other pH buffer. In order to provide similar experiment settings for coacervate preparation, for subsequent experiments, pH buffer 4.5 was chosen for immobilization of GA into sensor chip (Supplementary materials, Fig. S2a).

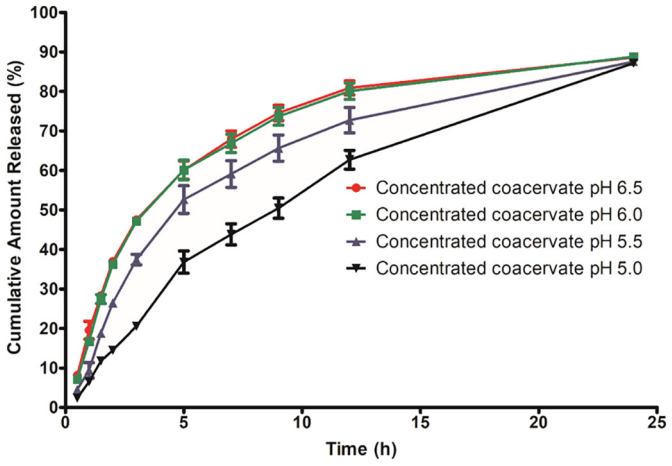

Fig. 4. In vitro release profiles of BSA from freeze-dried coacervates prepared at different pH values.

3.2.2. Immobilization

The GA immobilized on the sensor chip had a RU of 2242.6, which was calculated by subtracting the reference RU (Supplementary materials Fig. S2b) from the sensing RU (Supplementary materials Fig. S2c). The sensor chip promotes the binding of protein onto the surface via NH_2, COOH, CHO, and OH. The main amino acids in gelatin are glycine and proline. These amino acids can form covalent bonds with the gold sensor surface. The result with the least difference between the regeneration RU and the immobilized RU was chosen for the subsequent kinetics studies. In order to reuse the sensor chip, the analyte bound to the surface ought to be removed while the ligand remains intact. Regeneration value was generated based on the percentage value difference between the initial immobilized values upon regeneration.

3.2.3. Binding and kinetic tests

For binding and kinetics study, 160 μM BSA was injected into the cell immobilized with 0.5 μM GA (Supplementary materials Fig. S3a). The regeneration value of 3% was obtained using the regeneration buffer (PBS at pH 7.22) (Supplementary materials, Table S2). The increased alkalinity of buffer is too harsh to remove the bound analytes with the RU lower than the initial baseline. In contrast, regeneration buffer with increased acidity was too mild to remove the analyte. Optimal regeneration with regeneration less than 5% shows that the bound analytes were dissociates from the sensor chip surface and the surface can be reused for subsequent assay. High RU value of 2120 at this condition could decrease the association rate of BSA to the GA immobilized on the sensor chip due to mass transport limitation. Consequently, the binding interaction will be limited and the kinetic data for binding will not be reliable [33]. Upon reduction of the molarity of BSA to 40 nM, the RU decreased to 650. Hence, serial dilution from 40 nM of BSA was used in the kinetics analysis.

2 μM of SA was injected into the cell immobilized with 0.5 μM of GA and the RU was 150 after subtracting the reference cell value

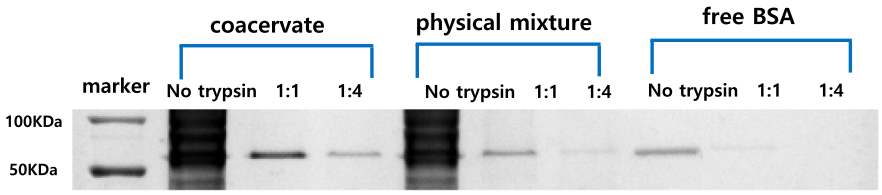

Fig. 3. Trypsin digestion of BSA in GA:SA (4:1) coacervate (Lanes 1–3), in physical mixture (Lanes 4–6), and in free solution (Lanes 7–9) at varying ratios of BSA to trypsin. (Marker: Lane 0).

Table 2
Association and dissociation constant of BSA to GA determined by SPR.

Concentration (nM)	Ka (1/Ms) association rate constant	K_D equilibrium dissociation constant/affinity constant (M)	Kd (s^{-1})
5	1.872e+6	1.454E−10	2.7218E−4
10	1.885e+6	1.444E−10	2.7219E−4
20	2.884e+6	9.425E−11	2.7181E−4
30	4.846e+6	5.610E−11	2.7186E−4
40	2.75e+7	9.86E−12	2.7110E−4

(Supplementary materials Fig. S3b). Although BSA had lower molarity than SA, the binding RU was higher than SA at the same molarity of GA. It suggests that the affinity of BSA to GA is higher than that of SA to GA. Regeneration of SA and BSA differed at each regeneration buffer (Supplementary materials, Table S2). The regeneration buffer pH to generate the minimal regeneration properties of less than 5% was pH 6.88 to 7.22 for SA and BSA, respectively. The minimum molarity required to reach the interaction between SA and GA was 0.125 μM whereas the minimum can be as low as 1 nM for BSA (data not shown). Interactions between polysaccharides were reported previously using SPR biosensor [34,35]. Those studies suggested selective adsorption between carbohydrates. The SPR studies in this study support the interactions between biopolymers in mimicking the formulation of complex coacervate.

For kinetic study using SPR biosensor, RU range below 600 is often recommended [36]. Kinetics analysis was carried out for BSA at 40 nM. RU at approximately 650 was detected using the SPR biosensor. Using various molarity of BSA, Ka value was generated based on the 1:1 local fit model (Supplementary materials Fig. S4a, Table 2). Association increased proportionally as the concentration of BSA increased. The association and dissociation constants of SA to GA are shown in Supplementary materials Fig. S4b. The association rate to GA was faster with BSA than with SA while the dissociation rate was slower with SA. It may suggest that the electrostatic interactions triggered by pH change were stronger between BSA and GA than between SA and GA. Maximum RU binding and chi values of BSA and SA to GA respectively are shown in Table S4. The SPR biosensor results suggest that SPR can be a useful analytical tool to investigate coacervate formation between various polymers especially during the formulation stage.

SPR binding study did not show significant interaction between GA and EGF when tested in the experimental settings similar to those used to examine the interaction between GA and BSA. Poor encapsulation efficiency of EGF coacervate was consistent with the weak interaction between EGF with GA observed in SPR system. Interactions of EGF with other polymers remain unknown and would be an interesting subject for further study using SPR.

SPR binding study appears to delineate the contribution of one-dimensional interaction among polymer molecules in coacervation and the protein of interest to encapsulate. Table 3 compares the physicochemical properties of BSA and EGF. Difference between BSA and EGF in binding affinity to GA cannot be attributed to the difference in the net charges since their pI values are similar, 4.7 [37] vs. 4.5 [38]. The zeta potential of BSA was less negative than that of EGF in the present study, whereas similar values were reported in the literature. If zeta potential were a main contributing factor to electrostatic binding to GA, EGF would exhibit better or at least similar binding to GA compared to BSA. Therefore, other factors appear to play a role in determining the electrostatic binding of BSA or EGF to GA. A number of previous studies have reported the importance of the effective charge, local surface charge density, or protein charge patches in coacervation or polyelectrolyte binding [11,28,39,40]. For example, coacervate complex of oppositely charge polymers and protein is related to the charge density of surface, molecular weight, and ionic strength [28]. Interaction of coacervate complex was also explained previously using the planar geometry [39]. Theoretically, interaction occurs if the surface charge density is above the critical value with the transition from non-interacting solution into a soluble complex. Protein charge patches account to formation of complexes between proteins of the like-charges [28]. Additionally, Böhme and Scheler reported that the effective charge of BSA determines the kinetics of the interaction with other charged molecules with dependence on pH [40]. In BSA, three domains composed of alpha-helices with varying surface charge densities are known as depicted in Table 3 [41]. Such structured local surface charges are not evident in the three dimensional structure of EGF. Taken together, we may speculate that the binding of BSA or EGF to GA is governed not by the net charge but by the local surface charge density of these molecules, and thus affects the encapsulation efficiency.

The present study is the first, to the best of our knowledge, to demonstrate the importance of local binding affinity in association with different encapsulation efficiency of two proteins with similar net charges in a given complex coacervate system.

4. Conclusions

We have developed a drug delivery system based on coacervates composed of GA and SA to deliver the protein of interest. The present coacervate system can be used to achieve controlled release up to 24 h. BSA encapsulated in the system was protected from trypsin digestion, which demonstrates that the present approach will be useful especially in the topical delivery of protein, circumventing proteolytic degradation in the chronic wounds. Binding and kinetic studies using SPR biosensor have provided indispensable information for coacervation by unraveling the interactions between polymers and protein. The results of EGF studies suggested that GA was not a suitable polymer

Table 3
Physiochemical properties of BSA and EGF.

Component	BSA	EGF
Molecular weight (kDa)	66	6
pI [37,38]	4.7	4.5
Zeta potential[a]	−4.75	−11.3
Zeta potential in PBS buffer [38,42]	−12.91	−11.6
Amino acids [43,44]	583	53
Disulfide bond [43,44]	17	3
3D structure [45,46]	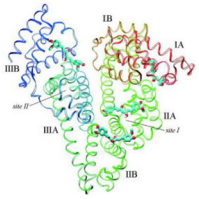	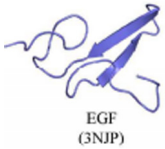 EGF (3NJP)

[a] Measured using Zetasizer Nano-ZS (Materials and methods: Section 2.2.2).

for EGF encapsulation, and therefore, further investigation would be needed to find suitable polymer systems for improved encapsulation efficiency.

Acknowledgement

This work was supported in part by the Korean Ministry of Trade Industry and Energy [No. 10047890] and National Research Foundation of Korea [NRF-2017R1D1A1B03031548].

Declaration of interest

The authors declare no conflicts of interest.

Appendix A. Supplementary data

Supplementary data to this article can be found online at https://doi.org/10.1016/j.ijbiomac.2018.05.093.

References

[1] D.R. Yager, S.M. Chen, S.I. Ward, O.O. Olutoye, R.F. Diegelmann, I. Kelman Cohen, Ability of chronic wound fluids to degrade peptide growth factors is associated with increased levels of elastase activity and diminished levels of proteinase inhibitors, Wound Repair Regen. 5 (1997) 23–32.
[2] F. Grinnell, C.H. Ho, A. Wysocki, Degradation of fibronectin and vitronectin in chronic wound fluid: analysis by cell blotting, immunoblotting, and cell adhesion assays, J. Invest. Dermatol. 98 (1992) 410–416.
[3] H.-C. Lau, A. Kim, Pharmaceutical perspectives of impaired wound healing in diabetic foot ulcer, J. Pharm. Investig. 46 (2016) 403–423.
[4] K. Ulubayram, A.N. Cakar, P. Korkusuz, C. Ertan, N. Hasirci, EGF containing gelatin-based wound dressings, Biomaterials 22 (2001) 1345–1356.
[5] H. Li, N.R. Johnson, A. Usas, A. Lu, M. Poddar, Y. Wang, J. Huard, Sustained release of bone morphogenetic protein 2 via coacervate improves the osteogenic potential of muscle-derived stem cells, Stem Cells Transl. Med. 2 (2013) 667–677.
[6] N.R. Johnson, T. Ambe, Y. Wang, Lysine-based polycation: heparin coacervate for controlled protein delivery, Acta Biomater. 10 (2014) 40–46.
[7] J.J. Hicks, J.L. Rocha, H. Li, J. Huard, Y. Wang, M.V. Hogan, Sustained release of bone morphogenetic protein 2 via coacervate improves muscle derived stem cell mediated cartilage regeneration in MIA-induced osteoarthritis, Orthop. J. Sports Med. 4 (2016) (2325967116S2325900152).
[8] H. Chu, J. Gao, C.-W. Chen, J. Huard, Y. Wang, Injectable fibroblast growth factor-2 coacervate for persistent angiogenesis, Proc. Natl. Acad. Sci. U. S. A. 108 (2011) 13444–13449.
[9] H. Chu, C.-W. Chen, J. Huard, Y. Wang, The effect of a heparin-based coacervate of fibroblast growth factor-2 on scarring in the infarcted myocardium, Biomaterials 34 (2013) 1747–1756.
[10] W.C. Chen, B.G. Lee, D.W. Park, K. Kim, H. Chu, K. Kim, J. Huard, Y. Wang, Controlled dual delivery of fibroblast growth factor-2 and interleukin-10 by heparin-based coacervate synergistically enhances ischemic heart repair, Biomaterials 72 (2015) 138–151.
[11] S. Kim, J. Huang, Y. Lee, S. Dutta, H.Y. Yoo, Y.M. Jung, Y. Jho, H. Zeng, D.S. Hwang, Complexation and coacervation of like-charged polyelectrolytes inspired by mussels, Proc. Natl. Acad. Sci. U. S. A. 113 (2016) E847–E853.
[12] F. Comert, A.J. Malanowski, F. Azarikia, P.L. Dubin, Coacervation and precipitation in polysaccharide–protein systems, Soft Matter 12 (2016) 4154–4161.
[13] C.-H. Xue, M.-M. Shi, H.-Z. Chen, G. Wu, M. Wang, Preparation and application of nanoscale microemulsion as binder for fabric inkjet printing, Colloids Surf. A Physicochem. Eng. Asp. 287 (2006) 147–152.
[14] J. Lazko, Y. Popineau, J. Legrand, Soy glycinin microcapsules by simple coacervation method, Colloids Surf. B: Biointerfaces 37 (2004) 1–8.
[15] J. Wu, J. Ye, J. Zhu, Z. Xiao, C. He, H. Shi, Y. Wang, C. Lin, H. Zhang, Y. Zhao, Heparin-based coacervate of FGF2 improves dermal regeneration by asserting a synergistic role with cell proliferation and endogenous facilitated VEGF for cutaneous wound healing, Biomacromolecules 17 (2016) 2168–2177.
[16] M.S. Lee, T. Ahmad, J. Lee, H.K. Awada, Y. Wang, K. Kim, H. Shin, H.S. Yang, Dual delivery of growth factors with coacervate-coated poly (lactic-*co*-glycolic acid) nanofiber improves neovascularization in a mouse skin flap model, Biomaterials 124 (2017) 65–77.
[17] K.A. Black, D. Priftis, S.L. Perry, J. Yip, W.Y. Byun, M. Tirrell, Protein encapsulation via polypeptide complex coacervation, ACS Macro Lett. 3 (2014) 1088–1091.
[18] K. Okumura, Y. Kiyohara, F. Komada, S. Iwakawa, M. Hirai, T. Fuwa, Improvement in wound healing by epidermal growth factor (EGF) ointment. I. Effect of nafamostat, gabexate, or gelatin on stabilization and efficacy of EGF, Pharm. Res. 7 (1990) 1289–1293.
[19] K. Kawai, S. Suzuki, Y. Tabata, Y. Nishimura, Accelerated wound healing through the incorporation of basic fibroblast growth factor-impregnated gelatin microspheres into artificial dermis using a pressure-induced decubitus ulcer model in genetically diabetic mice, Br. J. Plast. Surg. 58 (2005) 1115–1123.
[20] K. Hori, C. Sotozono, J. Hamuro, K. Yamasaki, Y. Kimura, M. Ozeki, Y. Tabata, S. Kinoshita, Controlled-release of epidermal growth factor from cationized gelatin hydrogel enhances corneal epithelial wound healing, J. Control. Release 118 (2007) 169–176.
[21] V.-T. Nguyen, S.-C. Ko, G.-W. Oh, S.-Y. Heo, Y.-J. Jeon, W. Sun Park, I.-W. Choi, S.-W. Choi, W.-K. Jung, Anti-inflammatory effects of sodium alginate/gelatine porous scaffolds merged with fucoidan in murine microglial BV2 cells, Int. J. Biol. Macromol. 93 (2016) 1620–1632.
[22] S.R. Hong, S.J. Lee, J.W. Shim, Y.S. Choi, Y.M. Lee, K.W. Song, M.H. Park, Y.S. Nam, S.I. Lee, Study on gelatin-containing artificial skin IV: a comparative study on the effect of antibiotic and EGF on cell proliferation during epidermal healing, Biomaterials 22 (2001) 2777–2783.
[23] Y.H. Kim, Y. Tabata, Enhancement of wound closure by modifying dual release patterns of stromal-derived cell factor-1 and a macrophage recruitment agent from gelatin hydrogels, J. Tissue Eng. Regen. Med. 11 (2017) 2999–3013.
[24] C. Jinno, N. Morimoto, R. Ito, M. Sakamoto, S. Ogino, T. Taira, S. Suzuki, A comparison of conventional collagen sponge and collagen-gelatin sponge in wound healing, Biomed. Res. Int. 2016 (2016) 1–9.
[25] M. Rezvanian, M.C.I.M. Amin, S.-F. Ng, Development and physicochemical characterization of alginate composite film loaded with simvastatin as a potential wound dressing, Carbohydr. Polym. 137 (2016) 295–304.
[26] R. Raguvaran, B.K. Manuja, M. Chopra, R. Thakur, T. Anand, A. Kalia, A. Manuja, Sodium alginate and gum acacia hydrogels of ZnO nanoparticles show wound healing effect on fibroblast cells, Int. J. Biol. Macromol. 96 (2017) 185–191.
[27] U.A. Shinde, M.S. Nagarsenker, Characterization of gelatin-sodium alginate complex coacervation system, Indian J. Pharm. Sci. 71 (2009) 313.
[28] E. Kizilay, A.B. Kayitmazer, P.L. Dubin, Complexation and coacervation of polyelectrolytes with oppositely charged colloids, Adv. Colloid Interf. Sci. 167 (2011) 24–37.
[29] N. Devi, D. Hazarika, C. Deka, D. Kakati, Study of complex coacervation of gelatin A and sodium alginate for microencapsulation of olive oil, J. Macromol. Sci. A 49 (2012) 936–945.
[30] C. Elmer, A.C. Karaca, N.H. Low, M.T. Nickerson, Complex coacervation in pea protein isolate–chitosan mixtures, Food Res. Int. 44 (2011) 1441–1446.
[31] H. Bohidar, Coacervates: a novel state of soft matter: an overview, J. Surf. Sci. Technol. 24 (2008) 105–124.
[32] K. Rawat, H. Bohidar, Coacervation in biopolymers, J. Phys. Chem. Biophys. 4 (2014) 1.
[33] M. Murphy, L. Jason-Moller, J. Bruno, Using biacore to measure the binding kinetics of an antibody-antigen interaction, Current Protocols in Protein Science, John Wiley@Sons Inc, 2006.
[34] Q. Wang, J.-F. Wang, P.H. Geil, G.W. Padua, Zein adsorption to hydrophilic and hydrophobic surfaces investigated by surface plasmon resonance, Biomacromolecules 5 (2004) 1356–1361.
[35] K. Matsuura, R. Oda, H. Kitakouji, M. Kiso, K. Kitajima, K. Kobayashi, Surface plasmon resonance study of carbohydrate–carbohydrate interaction between various gangliosides and Gg3-carrying polystyrene, Biomacromolecules 5 (2004) 937–941.
[36] D. Andreu, P. Gomes, Binding of small peptides to immobilized antibodies: kinetic analysis by surface plasmon resonance, Current Protocols in Immunology, John Wiley@Sons. Inc, 2002.
[37] R. Li, Z. Wu, Y. Wangb, L. Ding, Y. Wang, Role of pH-induced structural change in protein aggregation in foam fractionation of bovine serum albumin, Biotechnol. Rep. 9 (2016) 46–52.
[38] N.A. Kim, D.G. Lim, J.Y. Lim, K.H. Kim, S.H. Jeong, Fundamental analysis of recombinant human epidermal growth factor in solution with biophysical methods, Drug Dev. Ind. Pharm. 41 (2015) 300–306.
[39] O. Evers, G. Fleer, J. Scheutjens, J. Lyklema, Adsorption of weak polyelectrolytes from aqueous solution, J. Colloid Interface Sci. 111 (1986) 446–454.
[40] U. Böhme, U. Scheler, Effective charge of bovine serum albumin determined by electrophoresis NMR, Chem. Phys. Lett. 435 (2007) 342–345.
[41] B. Jachimska, A. Pajor, Physico-chemical characterization of bovine serum albumin in solution and as deposited on surfaces, Bioelectrochemistry 87 (2012) 138–146.
[42] G. Yan, Y. He, G. Li, Y. Xiong, P. Song, R.-M. Wang, Bovine serum albumin metal complexes for mimic of SOD, J. Chem. Sci. 128 (2016) 1783–1788.
[43] B.A. Sampoli Benitez, E.A. Komives, Disulfide bond plasticity in epidermal growth factor, Proteins: Struct., Funct., Bioinf. 40 (2000) 168–174.
[44] V.A. Borzova, K.A. Markossian, N.A. Chebotareva, S.Y. Kleymenov, N.B. Poliansky, K.O. Muranov, V.A. Stein-Margolina, V.V. Shubin, D.I. Markov, B.I. Kurganov, Kinetics of thermal denaturation and aggregation of bovine serum albumin, PLoS One 11 (2016), e0153495.
[45] K.M. Naik, D.B. Kolli, S.T. Nandibewoor, Elucidation of binding mechanism of hydroxyurea on serum albumins by different spectroscopic studies, SpringerPlus 3 (2014) 360.
[46] D.R. Sudhakar, P. Kalaiarasan, N. Subbarao, Docking and molecular dynamics simulation study of EGFR1 with EGF-like peptides to understand molecular interactions, Mol. BioSyst. 12 (2016) 1987–1995.